Journal of Nuclear Materials 386–388 (2009) 475–478

Contents lists available at ScienceDirect

Journal of Nuclear Materials

journal homepage: www.elsevier.com/locate/jnucmat

Study of PM2000 microstructure evolution following FSW process

M.H. Mathon [a,*], V. Klosek [a], Y. de Carlan [b], L. Forest [c]

[a] Laboratoire Léon Brillouin (CEA-CNRS), CEA/Saclay, 91191 Gif-sur-Yvette, France
[b] Service de Recherches Métallurgiques Appliquées, CEA/Saclay, 91191 Gif-sur-Yvette, France
[c] LTA, CEA/ Saclay, 91191 Gif sur Yvette, France

A B S T R A C T

The materials reinforced by oxides dispersion, usually called ODS (Oxide Strengthened Dispersion), have a vast applicability because of their excellent mechanical resistance at medium and high temperatures. Their weldability is one of the technological issue which remain today. The Friction Stir Welding process is a means of welding which would make it possible to preserve the oxides dispersion in the metal matrix. As a solid-state joint process, Friction Stir Welding (FSW) joins metals by locally introducing frictional heat and plastic flow by rotation of the welding tool with resulting local microstructure changes. The local microstructure determines the weld mechanical properties. Therefore, it is important to investigate the relationship between the microstructure and the mechanical properties. In this work, the PM2000 steel microstructure in friction stir (FS) weld was studied by neutron scattering. The oxides size distribution evolution between the bulk and the weld was analyzed by SANS. Crystallographic texture variations during friction stir processing were investigated by neutron diffraction. Indeed, heating and severe plastic deformation can significantly alter the original texture and then affect the physical and mechanical properties. The texture was studied in different zones: in the bulk, in the thermo-mechanically affected zone (TMAZ) and is the heat-affected zone (HAZ) of the PM2000 alloy. Lastly, the stresses distribution after welding is a crucial parameter for the mechanical properties. Their variation prediction under FSW, taking into account of the microstructure evolution which occur during the process, is very delicate. The neutron diffraction allowed characterizing the distribution of the stresses in the different zones.

1. Introduction

The materials reinforced by oxide dispersion, usually called ODS (Oxide Dispersion Strengthened), have wide ranging applications because of their excellent mechanical resistance at medium and high temperatures. In particular, ODS steels are candidates for structural materials of next generation nuclear reactors [1,2]. It is now well-known that the improvement of their creep behaviour is due to a very high density of Y–Ti–O nm-scale precipitate phases which act as barriers to mobile dislocations and grain boundaries. To improve the mechanical properties, the oxides size distribution must be optimized: for a maximum precipitated volume fraction, the oxide size should be as small as possible.

Friction stir welding, a process invented at The Welding Institute (TWI) Cambridge [3], involves the joining of metals without fusion or filler materials. In the case of ODS alloys, this welding process has the advantage of avoiding the oxides dissolution but induces severe microstructure evolution. A typical FS weld consists of: a thermo-mechanically affected zone (TMAZ), which includes the dynamically recrystallized stir zone (SZ) and the deformed but not recrystallized surrounded region, the heat-affected zone (HAZ) and the unaffected base material (BM). The main objective of this work is to study the microstructure evolution induced by the FSW process in the PM2000 ODS steel. For this purpose, the size distribution of oxides has been determined by small angle neutron scattering in the different zones. Furthermore, the texture and residual stress were characterized by neutron diffraction.

2. Experimental

The studied material is PM2000, a commercial ODS steel manufactured by Plansee. Its chemical composition is Fe 19%Cr 5.5%Al 0.5%Ti 0.5%Y_2O_3. Its microstructure is composed of fine grains of size lower than 10 μm. Plates with a thickness of 1.3 mm were welded with the following conditions: the travelling speed and the rotating speed were 5 cm/min and 600 rpm, respectively. The force, normal to the plate surface, was fixed at 14 kN. The length and the diameter of the pin were 1.5 and 3 mm, respectively and its shoulder diameter is 12 mm. The tool was made of polycrystalline cubic boron nitride provided by Danstir.

* Corresponding author.
E-mail address: marie-helene.mathon@cea.fr (M.H. Mathon).

0022-3115/$ - see front matter © 2009 Elsevier B.V. All rights reserved.
doi:10.1016/j.jnucmat.2008.12.163

The oxides evolution was investigated by SANS experiments which were performed at the Laboratoire Léon Brillouin (CEA-CNRS), Saclay, on the PAXY small-angle instrument. The wavelength λ was 0.6 nm and the sample-to-detector distance (D) was 2 m, covering a scattering vector (**q**) range from 0.3 to 1.6 nm^{-1} ($q = 4\ \pi\ \sin\theta/\lambda$ where 2θ is the scattering angle). Measurements have been made at room temperature, under saturating magnetic field **H** (=2 T) perpendicular to the incident neutron beam direction, in order to separate the magnetic and nuclear scattering cross-sections [4]. In the case of ferromagnetic materials, the ratio between the scattered intensities measured in the directions perpendicular and parallel to the applied magnetic field, is defined by $A = 1 + (\Delta\rho_{magn}/\Delta\rho_{nucl})^2$, where $\Delta\rho_{nucl,magn}$ are the nuclear and magnetic contrasts, respectively. They depend on the difference of nuclear and magnetic scattering length densities between particles (precipitates) and matrix. This ratio gives information on the chemical composition of the particles.

The characterization of the crystallographic texture has been performed by neutron diffraction using the four-circles diffractometer 6T1 at the same laboratory. From the {1 1 0}, {2 0 0}, and {2 1 1} pole figures using a 5×5 (°) grid, the Orientation Distribution Functions were calculated using the LaboTex software from the LaboSoft company.

For these previous techniques, small samples were cut in different thermally or thermo-mechanically affected zones: in the stir zone (SZ) and in the affected surrounding zone (TMAZ). Further away from the weld, the heat-affected zone (HAZ) then the unaffected base metal were also investigated. The taking away in the TMAZ and HAZ zones were carried out on the two sides of the FSW joint: on the advancing side where the motion and rotation direction of the tool are in the same direction, and on the retreating side where the rotation direction is opposite to the tool movement.

The Residual stresses were determined by neutron diffraction on the G5.2 diffractometer at Laboratoire Léon Brillouin. A monochromatic neutron beam with $\lambda = 2.87$ Å was used to obtain diffraction peaks from {1 1 0} planes of the ferritic matrix at a diffraction angle 2θ close to 90°, thus providing an optimal combination between spatial and instrumental resolutions. A sampling volume of $1 \times 1 \times 1\ mm^3$ was used for strain measurements at mid-thickness of the welded plate along the longitudinal and transverse directions (assumed to be principal directions of the stress tensor). Due to the important texture in the base plates, the measured diffracted intensities for {1 1 0} planes were almost equal to zero (see Section 3.2) when the sample was oriented with the scattering vector along its normal direction. No strain measurement could thus be performed along the latter direction. Because of the very low thickness of the plates, the normal residual stresses were assumed to be fully relaxed (i.e. equal to zero).

Lattice spacings $d_{(1\,1\,0)}$ acted as a strain gauge [5], and the elastic strains ε_{ii} were evaluated from the shifts of the scattering angle 2θ with respect to its stress-free value $2\theta_0$: $\varepsilon_{ii} = \frac{d_{(110)} - d_{0,(110)}}{d_{0,(110)}} = \frac{\sin\theta_{0,(110)}}{\sin\theta_{(110)}} - 1$. The stress-free value $2\theta_0$ was measured 60 mm away from the weld centreline, assuming no residual stress at this distance from the weld. The strains were converted to stresses applying Hooke's law:

$\sigma_i = \frac{E_{(110)}}{1+\nu_{(110)}}\left[\varepsilon_i + \frac{\nu_{(110)}}{1-2\nu_{(110)}}(\varepsilon_x + \varepsilon_y + \varepsilon_z)\right]$, where $i = x, y, z$ corresponding to longitudinal, transverse and normal directions, respectively. $E_{(1\,1\,0)} = 224.7$ GPa is the Young modulus for {1 1 0} planes, and $\nu_{(110)} = 0.28$ the corresponding Poisson's ratio, both calculated for α-Fe applying Kröner model without texture [6]. Assuming $\sigma_z = 0$, it follows: $\varepsilon_z = (\varepsilon_x + \varepsilon_y)\ \nu_{(1\,1\,0)}/(\nu_{(1\,1\,0)} - 1)$.

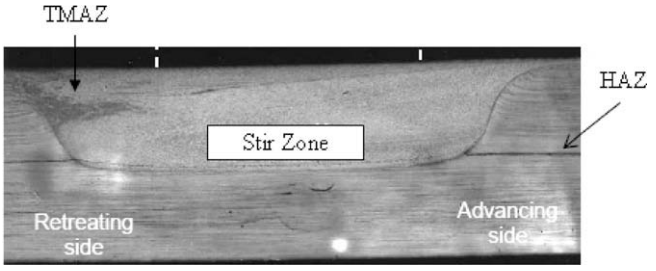

Fig. 1. MEB observation of the microstructure of the welded in PM2000 [7] (transverse cross-section).

3. Results

3.1. Characterization of yttrium oxide (Y_2O_3) by SANS

The SANS intensities presented on the Fig. 1, were measured on samples taken in the base material (BM), in the HAZ and at the interface of the TMAZ and stir zone (TMAZ/SZ) in the advancing side, in the stir zone and at the interface of the SZ and of the TMAZ in the retreating side. The SANS profiles analysis shows in the base material, two oxide populations whose average size is centred, respectively, on 15 and 5 nm. The total precipitated volume fraction is about 1%, each population accounts for 0.5%. This result is in agreement with TEM observations of Legendre et al. [7]. The A ratio equal to 2.7 is compatible with $Y_2Ti_2O_7$ oxides.

In the heat-affected zone, the two oxide populations are observed but the proportion of large particles increased (0.8%). This result shows the oxide growth in this zone. The A ratio for these particles is slightly higher than that in the BM (3.5). This increase can be explained by a small aluminium content in the oxides. For example, the A ratio associated to $Y_2(TiAl)_2O_7$ is equal to 3.7.

At the interface between the TMAZ and SZ, a quite similar behaviour is observed in the advancing and retreating zones. The volume fraction of observable particles decreases. This can be explained by the fact that some precipitates are too large to generate a scattered intensity seen in the explored angular range. Only the smallest particles are detected corresponding to a volume fraction of 0.5%.

The oxide growth is even more important in the stir zone. The SANS intensity is characteristic of particles larger than 10–20 nm and follows the Porod law ($I \sim (\Delta\rho_{magn}/\Delta\rho_{nucl})^2\ S_p/q^4$). From the scattered intensity, the total precipitate surface per unit of volume

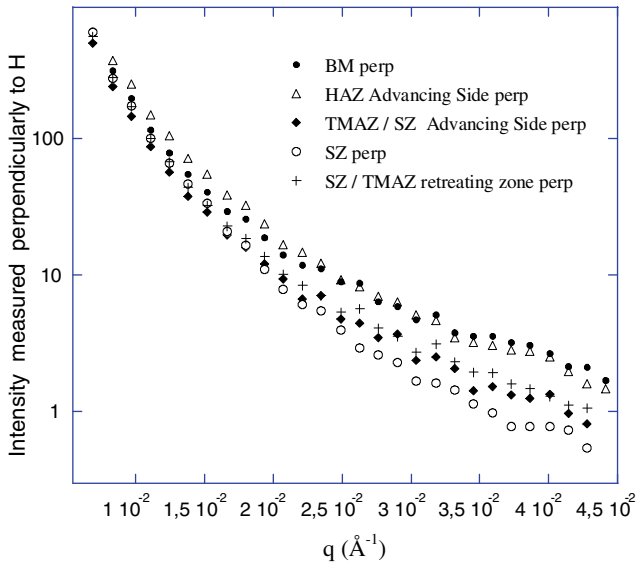

Fig. 2. Scattered intensity measured in SANS in PM2000 in the different zones around the weld.

can be deduced and is equal to 5.8×10^3 cm^2/cm^3. The A ratio is equal to 2.4 at the interface between the TMAZ and the SZ and in the stir zone. This value shows that the oxide chemical composition is different from that in the BM; it can correspond to $(YTi_{1-x}Al_x)_2O_3$ particles (see Fig. 2).

3.2. Evolution of the texture during the FSW process

The poles figures {1 1 0} measured on all the samples are presented Fig. 3. The base material presents a very sharp texture. The main component is {0 0 1} <1 1 0>; it corresponds to the maximum value of the Orientation Distribution Function (ODF) (1050 mrd). Some weak (levels from 3 to 5) reinforcements are observable in the ODF for the crystallographic orientations {1 1 1} <1 −2 1> and {2 2 1} <1 −1 0>. These components are characteristic of a cold rolling texture in bcc materials [8]. In the HAZ in the retreating zone, the {0 0 1} <1 1 0> reinforcement so high that in the base material is observed. The other orientations are slightly more marked, and we note the new components {2 0 1} <1 1 −2> and {1 0 1} <2 1 −2>.

In the TMAZ in advancing side, the same components as in the HAZ are observed but the sharpness of texture is reduced with a maximum ODF of 238 mrd. In the retreating side, the behaviour is quite similar but not as much marked (FDOC maximum value is equal to 832 mrd). The other component {2 0 1} <1 1 −2> is slightly weaker than in advancing side.

In the weld zone, the texture is weak and almost dispersed. The ODF maximum value is only 3.5 mrd and the maximum levels correspond to a residual {1 0 1} <2 1 −2> component.

3.3. Distribution of the residual stress

The obtained residual stresses along longitudinal and transverse directions are shown in Fig. 4. The observed stress profiles are typical of friction stir welding process, with a characteristic "M" shape [9], i.e. a tensile state in the TMAZ and HAZ, with local minima at the centre of the weld (corresponding to the TMAZ, and SZ), balanced by small compression away. The tensile peaks in the heat-affected zone are strongly asymmetric. For instance, values of residual longitudinal stresses reach 450 MPa in the advancing side, and only 320 MPa in the retreating side. This asymmetry in the longitudinal stresses was previously reported in friction stir welded aluminium alloys, and attributed to originate from a higher heat input on the advancing side due to the greater relative velocity between the tool and the workpiece [9]. Smaller asymmetry also appears on the transverse stress profile, but with higher values on the retreating side (up to 320 MPa) than on the advancing side (up to 250 MPa). At the centre of the weld, transverse stress tends to zero.

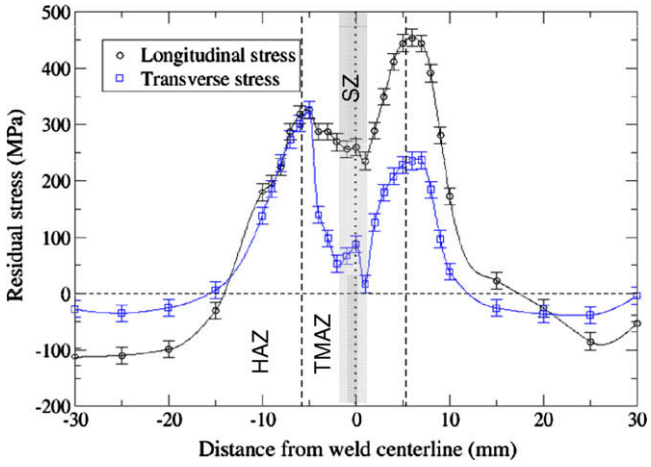

Fig. 4. longitudinal and transverse residual stresses versus distance from the weld centreline.

Longitudinal residual stresses exhibit the highest values, in good accordance with previous studies reported in stainless steels [10] or Al alloys [11,12]. However, the maximum longitudinal value appears to be quite low when compared to the base metal yield strength (900 MPa at 20 °C). Moreover, contrary to what is generally observed, transverse stresses obtained in the present study

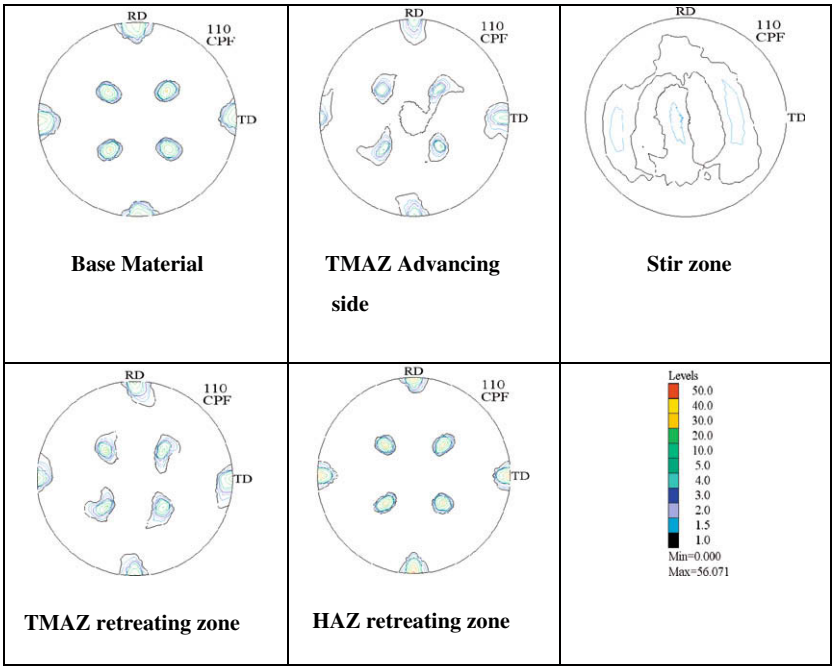

Fig. 3. {1 0 0} poles figures measured by neutron diffraction on PM2000 in the different zone after FSW process.

are also very high in the heat-affected zone. Both in Al alloys and stainless steels, FSW process is reported to induce rather small transverse stresses compared with longitudinal stresses, with almost no asymmetry [10,12]. The higher values of transverse stresses, and the lower values of longitudinal stresses obtained here may reflect the presence of strong intergranular stresses [13], resulting from plastic anisotropy of the bcc lattice and from the very sharp texture of the base material. Moreover, it should be noted that these values correspond to the average residual stress values through the whole thickness of the plates (the cubic gauge volume being tilted of 90° from the normal direction), and it is likely that differences and stress gradients, especially of transverse stresses, occur through the thickness [10].

4. Conclusion

This work gave a description of the microstructure evolutions in the various zones affected by the FSW process in the PM2000 alloy. The SANS technique clearly showed that the average sizes before FSW (5 and 15 nm) grow larger as one approaches the stir zone. In the nugget of the weld joint, the size of the particles is too large to allow quantifying their size and volume fraction. The base material has an extremely marked {0 0 1}<1 1 0> texture. This texture gradually disappears in TMAZ as the area approaches the weld zone. We observe an asymmetry between retreating and advancing side. The retreating side presents the same but less marked microstructure evolutions than in the advancing side.

Stress measurements showed an increase of the residual stresses in the weld zone, more important in the direction of the welding than in the transverse direction. In addition, the reached stress values are lower in the retreating side.

References

[1] R.L. Klueh, D.S. Gelles, S. Jitsukawa, A. Kimura, G.R. Odette, B. van der Schaaf, M. Victoria, J. Nucl. Mater. 307–311 (2002) 455.
[2] S. Jitsukawa, A. Kimura, A. Kohyama, R.L. Klueh, A.A. Tavassoli, B. van der Schaaf, G.R. Odette, J.W. Rensman, M. Victoria, C. Petersen, J. Nucl. Mater. 329–333 (2004) 39.
[3] W.M. Thomas, E.D. Nicholas, J.C. Needham, M.G. Murch, P. Temple-smith, C.J. Dawes, International Patent Application No. PCT/GB92/02203.
[4] M.H. Mathon, C.H. de Novion, J. de Physique IV (France) 9 (1999) 127.
[5] I.C. Noyan, J.B. Cohen, Residual Stress Measurement by Diffraction and Interpretation, Materials Research Engineering, Springer-Verlag, 1987.
[6] E. Kröner, Acta Metall. Mater. V9 (1961) 155.
[7] F. Legendre, S. Poissonet, P. Bonnaillie, L. Boulanger, L. Forest, Microstructural characterization of a friction stir welded oxide dispersion strenghtened ferritic steel alloy, these proceedings.
[8] F.J. Humphreys, M. Hatherly, Recrystallization and Related Annealing Phenomena, Pergamon, 1995.
[9] M.B. Prime, T. Gnäupel-Herold, J.A. Baumann, R.J. Lederich, D.M. Bowden, R.J. Sebring, Acta Mater. 54 (2006) 4013.
[10] A.P. Reynolds, W. Tang, T. Gnäupel-Herold, H. Prask, Scripta Mater. 48 (2003) 1289.
[11] W. Woo, H. Choo, D.W. Brown, Z. Feng, P.K. Liaw, Mat. Sci. Eng. A 437 (2006) 64.
[12] M. Peel, A. Steuwer, M. Preuss, P.J. Withers, Acta Mater. 51 (2003) 4791.
[13] D.G. Carr, M.I. Ripley, T.M. Holden, D.W. Brown, S.C. Vogel, Acta Mater. 52 (2004) 4083.